



Published in final edited form as:

*Biomacromolecules*. 2011 October 10; 12(10): 3549–3558. doi:10.1021/bm200763y.

## Directed intermixing in multi-component self-assembling biomaterials

Joshua Z. Gasiorowski<sup>a</sup> and Joel H. Collier<sup>a,b</sup>

<sup>a</sup>Department of Surgery, University of Chicago, 5841 S. Maryland Ave., Chicago, IL 60637

<sup>b</sup>Committee on Molecular Medicine, University of Chicago, 5841 S. Maryland Ave., Chicago, IL 60637

### Abstract

The non-covalent co-assembly of multiple different peptides can be a useful route for producing multifunctional biomaterials. However, to date such materials have almost exclusively been investigated as homogeneous self-assemblies, having functional components uniformly distributed throughout their supramolecular structures. Here we illustrate control over the intermixing of multiple different self-assembling peptides, in turn providing a simple but powerful means for modulating these materials' mechanical and biological properties. In beta-sheet fibrillizing hydrogels, significant increases in stiffening could be achieved using heterobifunctional cross-linkers by sequestering peptides bearing different reactive groups into distinct populations of fibrils, thus favoring inter-fibril cross-linking. Further, by specifying the intermixing of RGD-bearing peptides in 2-D and 3-D self-assemblies, the growth of HUVECs and NIH 3T3 cells could be significantly modulated. This approach may be immediately applicable towards a wide variety of self-assembling systems that form stable supramolecular structures.

### Keywords

peptide; fibril; extracellular matrix; tissue engineering; regenerative medicine; nanomaterials

### Introduction

The self-assembly of proteins, peptides, and peptide derivatives into hydrogels is becoming a prominent approach for constructing materials within diverse applications including cell delivery, tissue engineering, 3D cell culture, and biosensors.<sup>1–5</sup> The most extensively investigated systems to date have included peptide amphiphiles,<sup>6–8</sup> fibrillizing peptides,<sup>9–14</sup> systems that oligomerize through  $\alpha$ -helical coiled coils,<sup>15–18</sup> self-assembling proteins,<sup>19,20</sup> collagen-mimetic systems,<sup>21–23</sup> and polymer-peptide conjugates.<sup>24,25</sup> Collectively, these strategies to build supramolecular assemblies from predictably folding precursors have enabled the design of new biomaterials with unprecedented control over chemical, physical, and biological properties such as mechanics, nanostructure, and specific biological activity. In early reports, networks and hydrogels were created from a single molecular species capable of self-organizing,<sup>7,26,27</sup> but as the design of these materials has evolved, co-assemblies of multiple different peptides and proteins have increasingly been

\*Corresponding Author: Joel H. Collier, Ph.D., Assistant Professor, Department of Surgery and Committee on Molecular Medicine, University of Chicago, 5841 S. Maryland Ave. MC 5032, Chicago, IL 60637, collier@uchicago.edu.

Supporting Information Available: Mass spectra for all peptides used, additional TEM images of fibril species, hydrogel pH values, and mass spectra with additional HPLC fractions included. This material is available free of charge via the Internet at <http://pubs.acs.org>.

reported.<sup>20,28,29</sup> Such strategies incorporating more than one co-assembling molecule have largely been aimed at installing precise amounts of different functional domains into the matrices, for example cell binding ligands,<sup>30</sup> mineralization sites,<sup>7,31</sup> chemical groups for covalent capture,<sup>32</sup> or immune epitopes.<sup>33</sup>

To date, these multi-component co-assemblies have been constructed homogeneously. That is, functionalized derivatives of self-assembling molecules have been combined or diluted within backgrounds of unfunctionalized molecules, presumably providing uniformly intermixed co-assemblies. This has been achieved in a number of examples, among them peptide amphiphiles bearing cell binding, growth factor binding, and polymerization domains;<sup>6,34</sup>  $\beta$ -sheet fibrillizing peptides bearing cell attachment ligands or immune epitopes;<sup>9,28,35,36</sup> short aromatic peptides bearing cell attachment ligands;<sup>30</sup> and coiled-coil assemblies bearing fluorescence or affinity labels.<sup>29,37</sup> These systems offer excellent routes for precisely integrating multiple different functionalized components into hydrogels, through simple processes of mixing and aqueous self-assembly. However, although the clustering of ligands has been controlled previously via the inclusion of branched peptides,<sup>38</sup> to our knowledge the intermixing of multiple different molecular species has not been investigated as a direct means for controlling these materials' biological properties. With respect to mechanical properties, efforts have been made to cross-link and stiffen peptide self-assemblies,<sup>9,32,39</sup> but homogeneously applied chemistries have resulted primarily in *intra*-fibril cross-linking,<sup>9,32,40</sup> whereas *inter*-fibril interactions are likely to be significant determinants of gel viscoelasticity.<sup>41</sup> In the approach reported here, *inter*-fibril cross-linking is favored by first directing different chemical functionalities into mutually exclusive populations of fibrils and then subsequently reacting them with heterobifunctional cross-linkers.

As a natural inspiration for self-assembled materials, extracellular matrices (ECMs) exhibit a high degree of control over the intermixing of their molecular constituents. They are not homogeneous mixtures of glycoproteins, but highly organized assemblies with functional domains localized to specific sites within their protein networks. For example, in basement membranes, laminin-111 does not form randomly mixed co-assemblies with other basement membrane proteins; rather, it self-polymerizes into a laminin network, which interpenetrates within other networks of basement membrane glycoproteins such as type-IV collagen.<sup>42</sup> In turn, the spatial arrangement of laminin's matrix-binding or cell-binding domains then influences the cross-linking and cell-adhesive functions of the network, respectively.<sup>43-45</sup> Analogously, we sought to likewise influence the degree of intermixing or mutually exclusive self-assembly within co-assembling peptide systems in order to achieve a novel level of control over the cross-linking and cell-binding behaviors of the materials.

The peptides investigated in this study belong to a series of peptides that self-assemble into  $\beta$ -sheet-rich fibrils.<sup>26,27,46</sup> At concentrations in the range of 2–40 mM, they are initially soluble in water but can be induced to form hydrogels upon pH neutralization or the introduction of monovalent or divalent salts.<sup>28,32,46,47</sup> Owing to the prevalent use of these materials in biological applications, this gelation has commonly been achieved by adding physiological buffers such as phosphate buffered saline (PBS) or cell culture media.<sup>47,48</sup> One example of these types of peptides is Q11 (QKQFQFQFEQQ), a short peptide that is capable of forming fibrils either by itself or when synthesized in tandem with other functional peptide sequences.<sup>28,32,46,47</sup> This fibril-nucleating Q11 domain has been useful in previous work for co-assembling several different cell-binding ligands into multi-peptide gels without significant perturbation of the networks' fibrillar morphology.<sup>28,32,47</sup> The assembly of Q11 has tolerated the presence of a variety of short peptide ligands, including positively charged, negatively charged, hydrophobic, and hydrophilic ligands.<sup>28,32,33,47,48</sup> Here, we developed a strategy to either co-fibrillize multiple Q11-based peptides

("intermixed", Figure 1A and 1B) or maintain them in mutually exclusive fibril populations within hydrogels ("separately assembled", Figure 1C). The approach is based on specifying the point in the fibrillization process at which the peptides intermix. We hypothesized that if the peptides were allowed to form protofibrils together, they would continue to exist as mixed fibrils upon lateral assembly and gelation, owing to the significant stability of  $\beta$ -sheet fibrillar assemblies. If, in contrast, two or more different peptides were allowed to form protofibrils separately, we hypothesized that they would continue to be maintained in distinct fibril populations even when multiple different fibril types were subsequently mixed and gelled. We demonstrate this approach using  $\beta$ -sheet fibrillizing peptides, but the approach is likely to be broadly applicable for many different self-assembling systems, including peptide amphiphiles,  $\alpha$ -helical coiled coil systems,  $\beta$ -hairpins, proteins, and others that are based on kinetically stable supramolecular structures. The strategy also does not necessarily require the production of new self-assembling molecules, making it immediately employable within many of these systems.

## Materials and Methods

### Peptide synthesis

Peptide synthesis reagents were purchased from NovaBiochem. All peptides (Figure 1A) were synthesized on a 0.25 mmol scale using a CS Bio 136 automated peptide synthesizer on Rink amide AM resin using standard Fmoc protocols and activation with HBTU/HOBt, as previously described.<sup>28,32,47</sup> Peptides were double-coupled and cleaved/deprotected with standard cleavage cocktails, precipitated and washed five times with cold diethyl ether, dissolved in water, frozen, lyophilized on a Labconco freeze-drying system, and stored as lyophilized powders at  $-20^{\circ}$  C. Peptides used for cross-linking and TEM experiments were purified using a Varian ProStar HPLC, C18 reverse-phase columns, and water/acetonitrile gradients (Supplemental Figure 1). Peptide identities were confirmed with an Applied Biosystems Voyager-DE Pro MALDI-TOF mass spectrometer in linear detection mode (Supplemental Figure 2).

### Peptide mixing and fibril formation

Self-assembled peptide gels were produced by dissolving lyophilized peptides in water with resistivity greater than  $18.2\text{ M}\Omega$ , at a concentration of 30 mM unless otherwise noted. Solutions were incubated for time periods up to 24 hours to facilitate formation of protofibrils, and final gelation was induced by overlaying the peptide solutions with phosphate-buffered saline (PBS, 0.2 g/L KCl, 0.2 g/L  $\text{KH}_2\text{PO}_4$ , 8 g/L NaCl, 1.15 g/L  $\text{Na}_2\text{HPO}_4$ , pH 7.4). If cysteine-containing peptides were used, 1 mM Tris (2-carboxyethyl) phosphine hydrochloride (TCEP) was also added. This methodology has been previously described for Q11-based peptides containing a variety of different N-terminal ligands, including positively charged, negatively charged, hydrophilic, and hydrophobic ligands, and can be used to form gels within cell culture inserts, multiwell plates, or templates for oscillating rheometry.<sup>32,47</sup> Although protofibrils were produced during assembly in water, the solutions remained fluid prior to PBS addition, allowing the combination of protofibrils by pipetting and vortexing. Fibrils and gels containing multiple different peptides were prepared in two different ways: by mixing the peptides as dry powders as the first step in the process (Figure 1B), or by mixing them in water only after they had fibrillized (Figure 1C). Multiple peptides mixed as dry powders and allowed to co-fibrillize upon the addition of water are referred to as "intermixed" (Figure 1B), whereas peptides that were combined only after they had formed protofibrils are referred to as "separately assembled" (Figure 1C). In some experiments, Q11 peptides with two different N-terminal amino acid sequences were doped into backgrounds of unmodified Q11. In these cases, intermixed fibrils and gels were formed by combining all three peptides (the two functionalized Q11 peptides plus Q11

itself) as dry powders and proceeding as described above. Separately assembled functionalized fibrils were produced by mixing each functionalized peptide with Q11 in separate containers, then proceeding as described above after protofibril formation (Figure 1C).

### Circular Dichroism (CD)

Prior to analysis, peptides were rendered to a low aggregation state by dissolving them in neat TFA for 15 minutes, precipitating them and washing them with diethyl ether, and drying them in a vacuum desiccator. Peptides were separately assembled or intermixed in water, to form solutions having 10mM total peptide and a 9:1 molar ratio of Q11:ligand-bearing Q11 derivative. These solutions had a pH of 2.8 and were allowed to self-assemble in water for 24 hours. They were then diluted to a final concentration of 500  $\mu$ M in water for analysis. An Aviv Model 202 circular dichroism instrument (Lakewood, NJ) was used. Scans were run in triplicate with a 0.5 nm step size at 25° C. A water blank was subtracted from all samples.

### Electron microscopy

Transmission electron microscopy (TEM) with immunogold labeling was used to assess fibrillization and to quantify the intermixing of various peptides. Fibrils containing N-terminal biotin or myc tags (biotin-RGD-Q11 and myc-Q11, sequences in Figure 1A) were prepared as described above, and the dual labels were visualized on the fibrils using streptavidin-conjugated 5 nm gold nanoparticles and antibody-conjugated 15 nm gold nanoparticles, respectively. Staining was performed as previously described,<sup>47</sup> with the following modifications. Solutions containing 0.3 mM fibrillized peptides were adsorbed onto 200 mesh lacey carbon grids, blocked with 2% acetylated bovine serum albumin (BSA)/0.1% cold water fish skin gelatin, and placed onto a series of droplets containing 1) monoclonal mouse anti-myc antibody (Sigma cat# M4439, 1:4 in PBS), 2) goat anti-mouse IgG-15 nm gold particles (EMS cat# 25133) and streptavidin-5 nm gold particles (Invitrogen cat # A32360, all particles diluted 1:4 in PBS), and 3) 1% uranyl acetate in water. Triplicate PBS washes were performed between staining steps. Grids were analyzed with an FEI Tecnai F30 TEM, and fibril-bound particles were counted per unit length of each fibril. Densely entangled mats or networks of fibrils were excluded from the analysis because bound particles could not be reliably counted in those instances.

### Cross-linking and mechanical analyses

Gels were formulated with lysine-terminated and cysteine-terminated peptides (Figure 1A), either intermixed together within fibrils or segregated into different fibril populations. Stiffening in response to the application of an amine- and thiol-reactive heterobifunctional cross-linker, succinimidyl-([*N*-maleimidopropionamido]-ethyleneglycol)<sub>12</sub>, SM(PEG)<sub>12</sub>, was then investigated. Gels were cast in molds to facilitate rheometric analysis, as previously described.<sup>28,32,47,49</sup> All gels for rheometric analysis contained 30 mM total peptide, with 1.5 mM of Lys-Q11, Cys-Q11, or both, the balance being Q11. With the exception of the separate or combined protofibrillization of initial peptide mixtures in water, all other steps were consistent between the two experimental groups, including pipetting and vortexing. Sham vortexing steps were conducted on the intermixed samples so as to control for any possible influence of shear. For pH neutralization prior to the addition of SM(PEG)<sub>12</sub>, gels were subjected to up to 8 PBS washes, 2 mL each, 30 minutes apart, and pH was monitored with a micro pH electrode inserted into the gel. Prior to cross-linking, gels were treated with 5 mM TCEP in PBS for 30 minutes and washed three times with 2 mL PBS. Gels were then cross-linked by overlaying with 10 mM SM(PEG)<sub>12</sub> (Thermo Scientific cat# 22112) in PBS for 24 hours, applied within a silicone well temporarily affixed to the slide. Gels not subjected to cross-linking were only overlaid with PBS.

Viscoelasticity of the slide-mounted, template-cast gels was measured using a Bohlin Gemini rheometer fitted with an 8 mm parallel plate (Malvern Instruments, Worcestershire, UK). To measure the viscoelastic properties of protofibril solutions, 80  $\mu$ l of sample was pipetted onto the bottom plate. Gap distances were about 0.8 mm for solutions and 1.0–1.2 mm for gels. A chamber was utilized to control evaporation. Storage and loss moduli were recorded at frequencies from 0.01–10 Hz at 0.2% strain and 25°C. Cross-linking reactions were also monitored with HPLC, by disassembling gels in neat trifluoroacetic acid for 3 minutes and eluting them on a C18 reverse-phase HPLC column using a 15–100% water-acetonitrile gradient, as described previously.<sup>47</sup> Fractions were collected and analyzed by MALDI-TOF mass spectrometry on a Voyager-DE PRO instrument, using  $\alpha$ -cyano-4-hydroxycinnamic acid as the matrix. Mass accuracy was determined with angiotensin II and insulin B chain standards (Sigma-Aldrich, St. Louis, MO)

### Cell Culture in 2-D and 3-D

For 2-dimensional experiments, primary human umbilical vein endothelial cells (HUVECs) were utilized. Prior to seeding onto peptide gels, HUVECs were maintained and subcultured in Single Quot supplemented EGM-2 medium at 37°C and 5% CO<sub>2</sub> in T-75 flasks according to the supplier's protocols. EGM-2 media, HUVECs, and culture reagents were purchased from Lonza. Gels were produced in a similar fashion as the rheometry experiments, except that 80  $\mu$ l peptide solutions were pipetted into 48-well tissue culture polystyrene plates instead of onto glass slides. Total peptide concentration was maintained at 30 mM. HUVECs were trypsinized from the flasks and  $1 \times 10^4$  cells were seeded onto the top of each gel. To assess cell growth, after 3 days of incubation MTS assays (Promega Cat# G3582) were performed as previously described and according to the manufacturer's protocol.<sup>32,47</sup> Sample values were blanked against negative control wells that contained identical gel formulations without cells. Additionally, a positive control well with cells plated onto tissue culture polystyrene was used to assess proper functioning of the assay. For visual evidence of live cells, HUVECs were also stained with calcein-AM for 30 minutes and imaged using a Zeiss MRm AxioCam mounted on an Axiovert 100 fluorescence microscope. For 3-dimensional experiments, NIH 3T3 fibroblasts were utilized. They were maintained in T-75 flasks containing Dulbecco's Modified Eagle's Medium (DMEM) supplemented with 10% fetal bovine serum and L-glutamine. For suspension in peptide gels,  $2 \times 10^4$  cells in 10  $\mu$ l were mixed with 80  $\mu$ l of 30 mM peptide in water. The solutions were then immediately pipetted into 48-well plates, and 400  $\mu$ l of media was gently added on top of the fibril/cell solution to induce gelation. MTS assays were performed as above after 3 days.

### Statistical Analysis

Fisher's Exact Test was utilized to determine significance in the gold labeling experiments. Cell culture experiments were performed with triplicate gels, with significance determined by paired t-tests.

## Results

### Soluble protofibrils as intermediates in the fabrication of intermixed or separately assembled gels

The goal of the work described here was to control how multiple  $\beta$ -sheet fibrillizing peptides co-assembled, to form either homogeneously mixed fibrils, where each individual fibril would be composed of a random mixture of all of the different peptides (Figure 1B), or to form segregated fibrils, where specified peptides would not intermix within the same fibril (Figure 1C). After developing such a strategy, we investigated how it could be employed to modulate both gel mechanics as well as bioactivity, by specifying the locations of cross-link points or cell-binding peptides, respectively, in fibrillar hydrogels. Our strategy was

predicated on achieving an initial degree of soluble protofibril formation without inducing full gelation of the peptides. This intermediate step was designed to allow solution-phase mixing of multiple different protofibrils, whether they were fully intermixed or had segregated peptides. Protofibrillization was brought about by incubating the peptides in water for 24 h at pH 2.8 (Figure 2A). By TEM, it was observed that Q11 treated in this way formed soluble protofibrils, as did intermixed combinations of Q11 and N-terminally functionalized variants of Q11. Circular dichroism indicated that these protofibrils contained predominantly  $\beta$ -structure (Figure 2D). Fibrils derived from mixtures of Q11 and Cys-Q11, Lys-Q11, myc-Q11, or biotin-RGD-Q11 appeared morphologically similar, as did ternary combinations of the ligand-bearing peptides and Q11 (a complete set of images representing all peptide combinations studied is shown in Supplemental Figure 3). Concentrated solutions of protofibrils were fluid and easily pipetted. They exhibited storage moduli about 80-fold lower than the storage moduli of similarly concentrated fibrils gelled with PBS (Figure 2C).<sup>28</sup> They were clear and did not exhibit any signs of turbidity, and although they met a rheological definition of a gel (relative frequency insensitivity and  $G'$  significantly greater than  $G''$ ), they were easily mixed without exhibiting any gross heterogeneity, fragmentation, or phase separation, in effect exhibiting significant shear thinning behavior. This property could be subsequently exploited to combine formed protofibrils before inducing their lateral assembly into hydrogels (Figure 1). Upon application of PBS, the peptide solutions were transformed into gels, in the manner that has been published previously for Q11-based materials,<sup>29,47</sup> and the constituent fibrils exhibited a coarser structure, with thicker fibrils that stained more strongly with uranyl acetate (Figure 2B).

### Control over peptide intermixing

By first forming soluble protofibrils of defined composition and then mixing these protofibrils to form gels, we found that degree of intermixing or mutual exclusion of different co-assembled peptides could be strongly biased. Immunoelectron microscopy was used to observe the distribution of various functionalized Q11 peptides in the “intermixed” and “separately assembled” cases (Figure 3). In both cases, the functionalized peptides were doped into a background of Q11 (27 mM Q11, 3 mM total functional peptide; mixtures containing both functional peptides contained 1.5 mM of each), in order to produce fibrils that were morphologically similar, with a relatively low degree of functionalization (Figure 2A–B, Figure 3A–C). Fibrils were incubated with both 5 nm gold nanoparticles conjugated to streptavidin and an anti-myc primary antibody followed by 15 nm gold nanoparticles conjugated to a secondary antibody. Fibrils were then catalogued by TEM (Figure 3D–H) into fibrils that bound only biotin-specific particles (Figure 3A), fibrils that bound only myc-specific particles (Figure 3B), or fibrils that bound both types (Figure 3C). In parallel, fibril lengths were measured so that the number of particles per unit length could be recorded (Figure 3D–G).

Before assessing how peptide distributions changed with different mixing techniques, it was important to measure the extent of off-target binding that could occur with the immunoelectron microscopy technique. Fibrils containing only biotin-RGD-Q11 bound the smaller streptavidin-conjugated particles predominantly (Figure 3A, D, percentages in Figure 3H). Because there were no myc epitopes in these fibrils, the larger gold particles that bound to them represented the non-specific background level, 9% of the total signal. Similarly, fibrils containing only myc-Q11 bound the myc-specific 15 nm particles predominantly (Figure 3B, E, percentages in Figure 3H), with a somewhat higher amount (17%) of non-specific background staining. Together, these control groups indicated reasonable specificity of the labeling, with an average background level of 13% of the total signal. The spacing of particles on the fibrils ranged between 0.25 – 2.75 particles per 100 nm of fibril length for the biotin-containing fibrils, and 0.25 – 1.5 particles per 100 nm for

the myc-containing fibrils. Samples containing both myc-Q11 and biotin-RGD-Q11 showed distinct differences, depending on whether the two functionalized peptides had been intermixed or separately assembled. The most common fibril species in separately assembled samples were those that bound one particle type but not the other (Figure 3F, percentages in H). The percentage of fibrils binding both types of particles was only 10% in this case, slightly lower even than the average background labeling of the controls. We interpreted this finding to be strong evidence that distinct populations of functionalized fibrils could be produced and maintained if protofibrils were allowed to form before multiple peptides were mixed. Conversely, the most prevalent fibrils for the intermixed case were those that bound both 15 nm and 5 nm particles (Figure 3G, percentages in H). In this group, 44% of the fibrils bound both particles, constituting the majority species. It was interesting that although the degree of intermixing was significant, it was not complete, indicating that some degree of phase separation existed even when the peptides were induced to form protofibrils together. Nevertheless, the fibril distributions of the intermixed and separately assembled cases were highly different statistically, with a  $p$  value of  $2.8 \times 10^{-19}$  by Fisher's Exact Test.

### Differential intermixing can be used to modulate the mechanics of cross-linked gels

A number of factors collectively determine the mechanical behavior of self-assembled peptide gels, including fibril diameter, fibril length, individual fibril stiffness, and any lateral inter-fibril interactions, whether these lateral interactions are covalent (e.g. cross-linking), or non-covalent (e.g. bundling, electrostatic interactions, hydrophobic interactions). Our hypothesis for the work described here was that a self-assembled system favoring the formation of covalent interfibril cross-links would result in stiffer gels, compared to systems favoring intrafibril cross-links. We utilized co-assemblies analogous to the ones described in the previous section, exploiting the control we had acquired over peptide intermixing, to test this hypothesis. Experiments employed a commercially available heterobifunctional cross-linker commonly used in bioconjugate chemistry, succinimidyl-(*N*-maleimidopropionamido)-dodecaethylene glycol ester, SM(PEG)<sub>12</sub>, having an amine-reactive *N*-hydroxysuccinimide (NHS) ester on one terminus and a thiol-reactive maleimide on the other. Although this cross-linking reagent is not as chemically specific as other bioconjugation techniques such as native chemical ligation, “click”-type chemistries, oxime ligation, or others,<sup>29,32,50</sup> this otherwise straightforward chemistry allowed a simple proof-of-principle study investigating the influence of peptide intermixing on gel stiffening, using L- $\alpha$ -amino acid peptides and a widely available cross-linking reagent. To produce amine-functionalized fibrils, we incorporated Q11 peptides having N-terminal Lys residues (Figure 1A). Thiolated fibrils were produced by incorporating Q11 peptides with N-terminal Cys residues. Fibrils containing one, the other, or both functionalities exhibited indistinguishable morphologies by TEM (Figure 2A, 2B, Supplemental Figure 3). Intermixed and separately assembled Cys-Q11 and Lys-Q11-containing fibrils were produced as described in the methods, analogously to the fibrils described above in the TEM labeling experiments. Importantly, all steps except the intermixed or separate incubations in water were kept strictly identical between groups so as to control for any differences in timing or shear-induced thinning. All samples were incubated for exactly the same amount of time in each condition, and sham mixing steps were performed on the intermixed samples to account for the additional mixing and vortexing necessary for producing the separately assembled samples. In addition, because the selectivity of the cross-linker required a pH between 7.0–7.5,<sup>51</sup> the peptide gels were washed serially with PBS to neutralize pH, which was monitored with a needle-type pH probe inserted into the center of the gel. It was found that 6–8 serial washes were sufficient to ensure pH neutralization (from pH 2.8 in water to pH 7.4 within a gel) (Supplemental Figure 4).

From the outset of the rheometry experiments, it was observed that the gels under investigation were somewhat stiffer than previously studied peptide-based gels. Q11 gels containing 30 mM peptide had a storage modulus of about 50 kPa at 0.1 Hz, stiffer than previous reports of Q11 gels having the same peptide concentration but storage moduli of about 20 kPa.<sup>47,52</sup> We found that the extended incubation times required for the intermixing studies allowed for additional gel assembly and stiffening. Gels prepared with similar incubation times compared to previous studies (0.5–24 h in water followed by 2 h under the PBS layer) produced storage moduli around 20 kPa, whereas gels incubated for 24 h under the PBS layer produced storage moduli around 50–70 kPa (Figure 4A).

The type of intermixing did have a significant influence over the resultant mechanical properties of the cross-linked gels (Figure 5A and 5B). Upon application of the heterobifunctional cross-linker, the storage moduli of gels composed of separately assembled Cys-Q11 and Lys-Q11 fibrils more than doubled compared to Q11 gels reacted with the cross-linker, from 52 kPa to 123 kPa at 0.19 Hz. In contrast, intermixed gels containing Cys-Q11 and Lys-Q11 did not exhibit such stiffness upon application of SM(PEG)<sub>12</sub>, having storage moduli of only 70 kPa at 0.19 Hz (Figure 5B). Cross-linked gels containing only one of the functionalized peptides also did not exhibit the dramatic stiffening seen in the separately assembled case. Application of SM(PEG)<sub>12</sub> to gels containing only Q11 produced similar stiffnesses compared to non-cross-linked gels (Figure 4A, 5A, 5B), suggesting that any cross-linker that may have reacted with the internal Lys residue within the Q11 sequence had minimal influence over storage modulus. The modest increase in the stiffness of gels containing only one of the two N-terminally functionalized peptides may indicate some degree of non-specific reactivity towards the maleimide or NHS groups, or conjugation between the internal Lys residue of Q11 and the N-terminal amino acids. In an effort to circumvent the possibility of the internal Lys of Q11 reacting with the cross-linker, a new peptide was synthesized substituting this residue with arginine, but it was found that this modified Lys3→Arg Q11 peptide was poorly soluble in water (not shown). However, even in the face of such opportunities for non-specific reactions, the separately assembled group exhibited a clear increase in stiffening beyond all other gel types, most notably the intermixed, which contained exactly the same concentrations of Cys- and Lys-terminated peptides but were not sequestered fully into mutually exclusive populations. Given the significant stiffening achieved in this simple system with imperfect specificity, it is possible that even greater matrix stiffening may be achieved using more chemoselective approaches.<sup>29,32,50</sup>

To monitor the formation of PEG-modified peptides, HPLC was performed on gels disaggregated using neat TFA,<sup>47</sup> and MALDI mass spectrometry was performed on the fractions, together verifying the formation of covalent cross-links between Lys-Q11 and Cys-Q11 in separately assembled gels (Figure 5C). A molecule corresponding to Lys-Q11 and Cys-Q11 cross-linked via SM(PEG)<sub>12</sub> ( $[M+H]^+$   $m/z$  calc'd: 4726.7, found 4731.8) was detected among a series of PEGylated peptide products that as a group eluted between 34–44 min on C18 columns under 20–35% acetonitrile gradients (Figure 5C, solid red line). Gels not reacted with cross-linker lacked this series of SM(PEG)<sub>12</sub>-modified peaks (Figure 5C, dashed blue line). The expected Lys/Cys cross-linked peptides were found within the 37–38 minute fraction, along with Q11 modified with SM(PEG)<sub>12</sub>, presumably by reaction with the internal Lys of Q11 (Figure 5C, 5D, Supplemental Figure 5). The other PEGylated peaks corresponded to Lys-Q11, Cys-Q11, and Q11, each individually reacted with SM(PEG)<sub>12</sub>, as well as Q11 cross-linked to Cys-Q11 via SM(PEG)<sub>12</sub> (See Supplemental Figure 5). Fragmentation of the PEGylated peptides was minimized by loading TFA-disaggregated gels onto C18 columns immediately upon dissolution, but some of the diversity in the PEGylated peaks may reflect the lability of these molecules in neat TFA, which was increasingly observed with more prolonged incubation (not shown).



## Differential intermixing can be used to modulate cell responses to self-assembled peptide matrices

Having illustrated that peptide intermixing could be employed as a simple means for modulating the mechanics of self-assembled peptide gels, we next sought to apply the same methods to control ligand positioning in self-assembled culture matrices. The density of adhesive ligands within a substrate can influence the clustering of integrins and the assembly of focal adhesions, which in turn can modulate cell adhesion, migration, and phenotype.<sup>53,54</sup> Having found that peptide intermixing could provide a direct means for tuning the mechanical properties of peptide hydrogels, we hypothesized that an analogous approach could be used to modulate the behavior of cells in contact with the materials, by specifying the intermixing of RGD-bearing Q11 peptides within a background of unmodified Q11. Indeed, we found that when HUVECs were cultured on the surface of the gels, intermixed RGD ligands supported a significantly greater amount of cell growth over separately assembled formulations (Figure 6A, D, E). Both intermixed and separately assembled RGD ligands promoted HUVEC growth over gels without ligands or with scrambled RGD ligands, but it was greatest on intermixed gels, at a level similar to that exhibited by Geltrex™, a biological matrix produced by EHS mouse tumor cells. It is unlikely that differences in growth could be attributed to differences in fibril morphologies, owing to the morphological similarity between different ligand-bearing fibrils (Figure 2, Supplemental Figure 3). Previous investigations of fibrils containing RGD-Q11 and RDG-Q11 have also found similar morphologies.<sup>47</sup> Furthermore, even though stiffness has previously been found to be a significant modulator of HUVEC growth on Q11-based materials,<sup>32</sup> intermixed and separately assembled RGD-bearing gels had similar storage moduli (Figure 4C), making it unlikely that the difference in cell growth could be ascribed to differences in mechanical properties. Interestingly, in a three-dimensional culture model, the significant influence of intermixing was also observed. When NIH 3T3 cells were encapsulated within the peptide hydrogels, intermixed gels supported significantly greater cell growth compared to separately assembled gels (Figure 6F). These results, along with the cross-linking studies, illustrate that peptide intermixing within self-assemblies can be a simple, powerful, and easily applied point of control for modulating both the mechanical and biological properties of multi-component biomaterials.

## Discussion

This strategy should be applicable within any self-assembling system in which an intermediate level of assembly can be achieved prior to the final mixing of all constituents. For Q11-based peptides, this intermediate assembly was achieved in aqueous solutions lacking the ionic strength necessary to form a gel. In pure water, Q11 and its functional derivatives formed soluble fibrils capable of preventing any subsequent exchange or intermixing of peptides as the fibrils were cast into hydrogels. Other systems which may exhibit similar assembly pathways include peptide amphiphiles,<sup>7</sup>  $\beta$ -hairpins,<sup>13,55</sup> other  $\beta$ -sheet fibrillizing peptides,<sup>26,27</sup> and short aromatic self-assembling peptides,<sup>30</sup> for which the reported approach should be directly applicable. More dynamic systems such as self-assembling proteins,<sup>20</sup> or coiled coil-based materials<sup>56</sup> may also benefit from directed intermixing, provided their assemblies are constructed using strategies that minimize dynamic rearrangement.<sup>19,57,55</sup> Within such materials, control over intermixing opens up interesting avenues for investigation, allowing a unique level of control over the spatial positioning of different ligands or functional domains. We show here that intermixing can significantly influence the mechanical properties and biological properties of co-assemblies as examples of this principle, but the approach may be generally useful for studying or exploiting subtler cell-matrix interactions. These might include how spatial relationships between multiple integrin ligands influence cell behavior,<sup>58,59</sup> or how synergies between

integrin ligands and growth factor binding sites depend on the macromolecular connectivity between them.<sup>60</sup>

In the  $\beta$ -sheet fibrillizing peptide system reported here, the separately assembled groups maintained strict sequestration of different functional domains in separate populations of fibrils, with mixed fibrils being undetectable above background. In contrast, the intermixed groups were not quantitatively intermixed, exhibiting a sizeable fraction of unmixed fibrils. A reasonable explanation may be that partially assembled peptide fibrils or seeds of oligomeric peptides could have existed in the lyophilized peptide stocks, which could have produced a population of fibrils that could not become intermixed. Still, nearly half of the fibrils from the intermixed samples contained both labels, and this level of intermixing minimized the stiffening achievable with the heterobifunctional cross-linker, presumably by allowing intrafibril cross-linking rather than interfibril cross-linking. In addition, it is possible that the ligands or chemical functionalities could have been differentially displayed or buried within the fibrils for the intermixed versus separately assembled case, and this could have contributed to the biological and mechanical effects observed. However, no overt differences in fibril morphology were measured that would suggest such a disruption of assembly by any of the components, and we kept the functional peptide density low (10% of total peptide) to minimize this issue.

Finally, the mechanisms responsible for the increased growth of cells cultured on or within gels containing intermixed RGD ligands remain unknown. Presumably, the spatial positioning of the adhesion ligands played a significant role. A regular, spatially homogeneous pattern of RGD ligands may maintain an optimal integrin engagement that is more conducive to efficient cell adherence, proliferation or differentiation.<sup>54,57</sup> Indeed, we observed consistent, spread HUVEC morphology when the cells were plated on gels with intermixed fibrils. It is also possible that the RGD ligand spacing on intermixed fibrils modulated focal adhesion complex arrangement, which could stimulate mitogenic pathways.<sup>61</sup> The precise spacing of available ligands on individual fibrils is as of yet unknown, but further investigation with ligand-bearing peptides may shed light on how such clustering is influenced by the mixing strategies outlined here, as well as the mechanisms by which such arrangements influence cell growth.

## Conclusions

We have demonstrated a method for producing self-assemblies of multiple peptides with control over the degree of intermixing between them, as quantified by TEM and immunogold labeling. Separately assembled fibrils could be used to generate hydrogels in which two different chemical functionalities were segregated into two discrete fibril populations, which in turn allowed a marked increase in the stiffening achievable with a heterobifunctional cross-linker. Additionally, RGD ligands intermixed within self-assembled gels resulted in significant increases in cell growth, both in 2-D and 3-D cultures, compared to gels with separately assembled ligands. The strategy outlined here should be broadly applicable within a variety of kinetically stable co-assemblies, providing an immediately accessible route for significantly adjusting their biological and mechanical properties without needing to develop new chemistries or molecules.

## Supplementary Material

Refer to Web version on PubMed Central for supplementary material.

## Acknowledgments

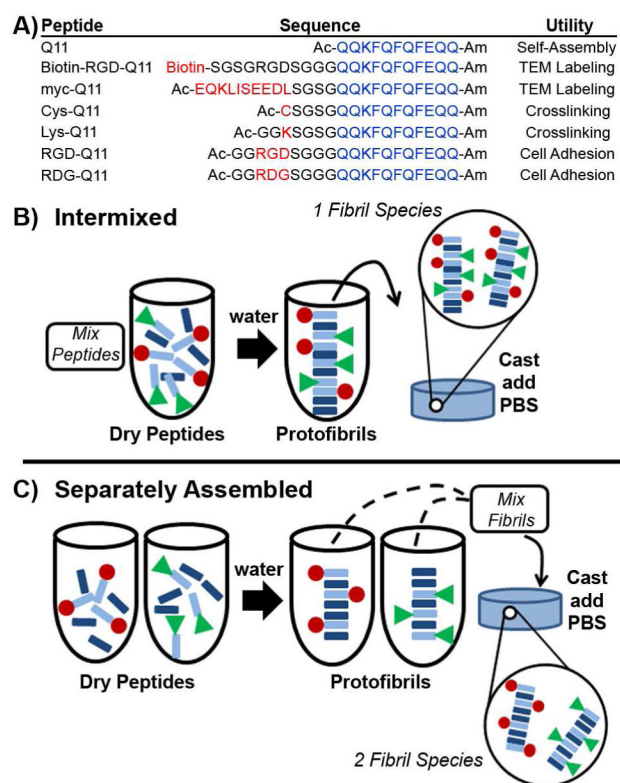
We thank Margaret Gardel for use of the rheometer and Philip Jung for helpful technical advice. TEM was performed at the University of Chicago Electron Microscopy core facility. This research was supported by the National Institutes of Health (NIBIB, 1R01EB009701; NCI, U54 CA151880), the Chicago Biomedical Consortium, and the National Science Foundation (CHE-0802286). The content is solely the responsibility of the authors and does not necessarily represent the official views of the National Institute of Biomedical Imaging and BioEngineering, the National Cancer Institute, or the National Institutes of Health.

## References

1. Aili D, Mager M, Roche D, Stevens MM. *Nano Lett.* 2011; 11:1401–1405. [PubMed: 20795711]
2. Davis ME, Motion JP, Narmoneva DA, Takahashi T, Hakuno D, Kamm RD, Zhang S, Lee RT. *Circulation.* 2005; 111:442–450. [PubMed: 15687132]
3. Genove E, Shen C, Zhang S, Semino CE. *Biomaterials.* 2005; 26:3341–3351. [PubMed: 15603830]
4. Lee RH, Seo MJ, Reger RL, Spees JL, Pulin AA, Olson SD, Prockop DJ. *Proc Natl Acad Sci U S A.* 2006; 103:17438–17443. [PubMed: 17088535]
5. Padin-Iruegas ME, Misao Y, Davis ME, Segers VF, Esposito G, Tokunou T, Urbanek K, Hosoda T, Rota M, Anversa P, Leri A, Lee RT, Kajstura J. *Circulation.* 2009; 120:876–887. [PubMed: 19704095]
6. Chow LW, Wang LJ, Kaufman DB, Stupp SI. *Biomaterials.* 2010; 31:6154–6161. [PubMed: 20552727]
7. Hartgerink JD, Beniash E, Stupp SI. *Science.* 2001; 294:1684–1688. [PubMed: 11721046]
8. Cui H, Webber MJ, Stupp SI. *Biopolymers.* 2010; 94:1–18. [PubMed: 20091874]
9. Aulisa L, Dong H, Hartgerink JD. *Biomacromolecules.* 2009; 10:2694–2698. [PubMed: 19705838]
10. Horii A, Wang X, Gelain F, Zhang S. *PLoS One.* 2007; 2:e190. [PubMed: 17285144]
11. Jayawarna V, Richardson SM, Hirst AR, Hodson NW, Saiani A, Gough JE, Ulijn RV. *Acta Biomater.* 2009; 5:934–943. [PubMed: 19249724]
12. Miroshnikova YA, Jorgens DM, Spirio L, Auer M, Sarang-Sieminski AL, Weaver VM. *Phys Biol.* 2011; 8:026013. [PubMed: 21441648]
13. Rajagopal K, Lamm MS, Haines-Butterick LA, Pochan DJ, Schneider JP. *Biomacromolecules.* 2009; 10:2619–2625. [PubMed: 19663418]
14. Galler KM, Aulisa L, Regan KR, D'Souza RN, Hartgerink JD. *J Am Chem Soc.* 2010; 132:3217–3223. [PubMed: 20158218]
15. Bromley EH, Sessions RB, Thomson AR, Woolfson DN. *J Am Chem Soc.* 2009; 131:928–930. [PubMed: 19115943]
16. Yang J, Xu C, Wang C, Kopecek J. *Biomacromolecules.* 2006; 7:1187–1195. [PubMed: 16602737]
17. Banwell EF, Abelardo ES, Adams DJ, Birchall MA, Corrigan A, Donald AM, Kirkland M, Serpell LC, Butler MF, Woolfson DN. *Nat Mater.* 2009; 8:596–600. [PubMed: 19543314]
18. Ryadnov MG, Woolfson DN. *Nat Mater.* 2003; 2:329–332. [PubMed: 12704382]
19. Petka WA, Harden JL, McGrath KP, Wirtz D, Tirrell DA. *Science.* 1998; 281:389–392. [PubMed: 9665877]
20. Wong Po Foo CT, Lee JS, Mulyasmita W, Parisi-Amon A, Heilshorn SC. *Proc Natl Acad Sci U S A.* 2009; 106:22067–22072. [PubMed: 20007785]
21. Russell LE, Fallas JA, Hartgerink JD. *J Am Chem Soc.* 2010; 132:3242–3243. [PubMed: 20058861]
22. Wang AY, Mo X, Chen CS, Yu SM. *J Am Chem Soc.* 2005; 127:4130–4131. [PubMed: 15783169]
23. Wang AY, Foss CA, Leong S, Mo X, Pomper MG, Yu SM. *Biomacromolecules.* 2008; 9:1755–1763. [PubMed: 18547103]
24. Grieshaber SE, Nie T, Yan C, Zhong S, Teller SS, Clifton RJ, Pochan DJ, Kiick KL, Jia X. *Macromol Chem Phys.* 2011; 212:229–239. [PubMed: 21359141]
25. Paderi JE, Panitch A. *Biomacromolecules.* 2008; 9:2562–2566. [PubMed: 18680341]

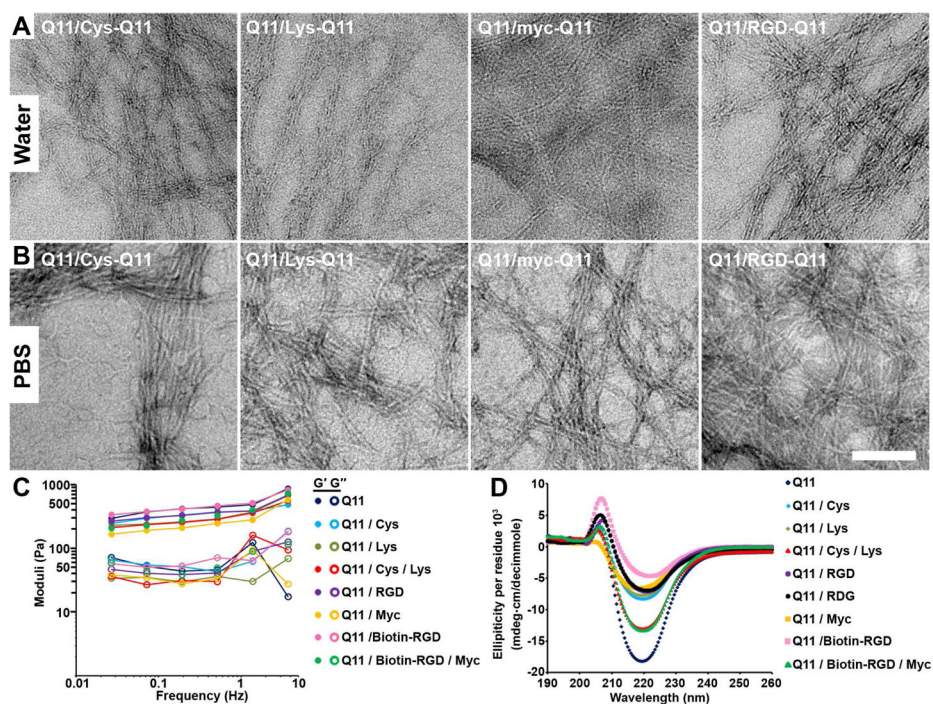
26. Aggeli A, Bell M, Boden N, Keen JN, Knowles PF, McLeish TCB, Pitkeathly M, Radford SE. *Nature*. 1997; 386:259–262. [PubMed: 9069283]
27. Zhang S, Holmes TC, DiPersio CM, Hynes RO, Su X, Rich A. *Biomaterials*. 1995; 16:1385–1393. [PubMed: 8590765]
28. Jung JP, Moyano JV, Collier JH. *Integr Biol (Camb)*. 2011; 3:185–196. [PubMed: 21249249]
29. Mahmoud ZN, Gunnoo SB, Thomson AR, Fletcher JM, Woolfson DN. *Biomaterials*. 2011; 32:3712–3720. [PubMed: 21353303]
30. Zhou M, Smith AM, Das AK, Hodson NW, Collins RF, Ulijn RV, Gough JE. *Biomaterials*. 2009; 30:2523–2530. [PubMed: 19201459]
31. Mata A, Geng Y, Henrikson KJ, Aparicio C, Stock SR, Satcher RL, Stupp SI. *Biomaterials*. 2010; 31:6004–6012. [PubMed: 20472286]
32. Jung JP, Jones JL, Cronier SA, Collier JH. *Biomaterials*. 2008; 29:2143–2151. [PubMed: 18261790]
33. Rudra JS, Tian YF, Jung JP, Collier JH. *Proc Natl Acad Sci U S A*. 2010; 107:622–627. [PubMed: 20080728]
34. Guler MO, Hsu L, Soukasene S, Harrington DA, Hulvat JF, Stupp SI. *Biomacromolecules*. 2006; 7:1855–1863. [PubMed: 16768407]
35. Gelain F, Bottai D, Vescovi A, Zhang S. *PLoS One*. 2006; 1:e119. [PubMed: 17205123]
36. Gras SL, Tickler AK, Squires AM, Devlin GL, Horton MA, Dobson CM, MacPhee CE. *Biomaterials*. 2008; 29:1553–1562. [PubMed: 18164758]
37. Mahmoud ZN, Grundy DJ, Channon KJ, Woolfson DN. *Biomaterials*. 2010; 31:7468–7474. [PubMed: 20638122]
38. Storrie H, Guler MO, Abu-Amara SN, Volberg T, Rao M, Geiger B, Stupp SI. *Biomaterials*. 2007; 28:4608–4618. [PubMed: 17662383]
39. Bakota EL, Aulisa L, Galler KM, Hartgerink JD. *Biomacromolecules*. 2011; 12:82–87. [PubMed: 21133404]
40. Rughani RV, Branco MC, Pochan DJ, Schneider JP. *Macromolecules*. 2010; 43:7924–7930.
41. Dagdas YS, Tombuloglu A, Tekinay AB, Dana A, Guler MO. *Soft Matter*. 2011; 7:3524–3532.
42. Kalluri R. *Nat Rev Cancer*. 2003; 3:422–433. [PubMed: 12778132]
43. Aumailley M, Wiedemann H, Mann K, Timpl R. *Eur J Biochem*. 1989; 184:241–248. [PubMed: 2506015]
44. Charonis AS, Tsilibary EC, Yurchenco PD, Furthmayr H. *J Cell Biol*. 1985; 100:1848–1853. [PubMed: 3997977]
45. Yurchenco PD, Cheng YS, Ruben GC. *J Biol Chem*. 1987; 262:17668–17676. [PubMed: 2961742]
46. Collier JH, Messersmith PB. *Bioconjug Chem*. 2003; 14:748–755. [PubMed: 12862427]
47. Jung JP, Nagaraj AK, Fox EK, Rudra JS, Devgun JM, Collier JH. *Biomaterials*. 2009; 30:2400–2410. [PubMed: 19203790]
48. Aggeli A, Bell M, Carrick LM, Fishwick CWG, Harding R, Mawer PJ, Radford SE, Strong AE, Boden N. *J Am Chem Soc*. 2003; 125:9619–9628. [PubMed: 12904028]
49. Sieminski AL, Was AS, Kim G, Gong H, Kamm RD. *Cell Biochem Biophys*. 2007; 49:73–83. [PubMed: 17906362]
50. Dirksen A, Dawson PE. *Bioconjug Chem*. 2008; 19:2543–2548. [PubMed: 19053314]
51. Hermanson, GT. *Bioconjugate Techniques*. 2. Academic Press, Inc.; 2008.
52. Jung JP, Gasiorowski JZ, Collier JH. *Biopolymers*. 2010; 94:49–59. [PubMed: 20091870]
53. Liu JC, Tirrell DA. *Biomacromolecules*. 2008; 9:2984–2988. [PubMed: 18826275]
54. Tang J, Peng R, Ding J. *Biomaterials*. 2010; 31:2470–2476. [PubMed: 20022630]
55. Nagarkar RP, Hule RA, Pochan DJ, Schneider JP. *Biopolymers*. 2010; 94:141–155. [PubMed: 20091872]
56. Jing P, Rudra JS, Herr AB, Collier JH. *Biomacromolecules*. 2008; 9:2438–2446. [PubMed: 18712921]
57. Liu B, Lewis AK, Shen W. *Biomacromolecules*. 2009; 10:3182–3187. [PubMed: 19919071]

58. Krammer A, Craig D, Thomas WE, Schulten K, Vogel V. *Matrix Biol.* 2002; 21:139–147. [PubMed: 11852230]
59. Puklin-Faucher E, Vogel V. *J Biol Chem.* 2009; 284:36557–36568. [PubMed: 19762919]
60. Hynes RO. *Science.* 2009; 326:1216–1219. [PubMed: 19965464]
61. Biggs MJ, Richards RG, Gadegaard N, Wilkinson CD, Oreffo RO, Dalby MJ. *Biomaterials.* 2009; 30:5094–5103. [PubMed: 19539986]



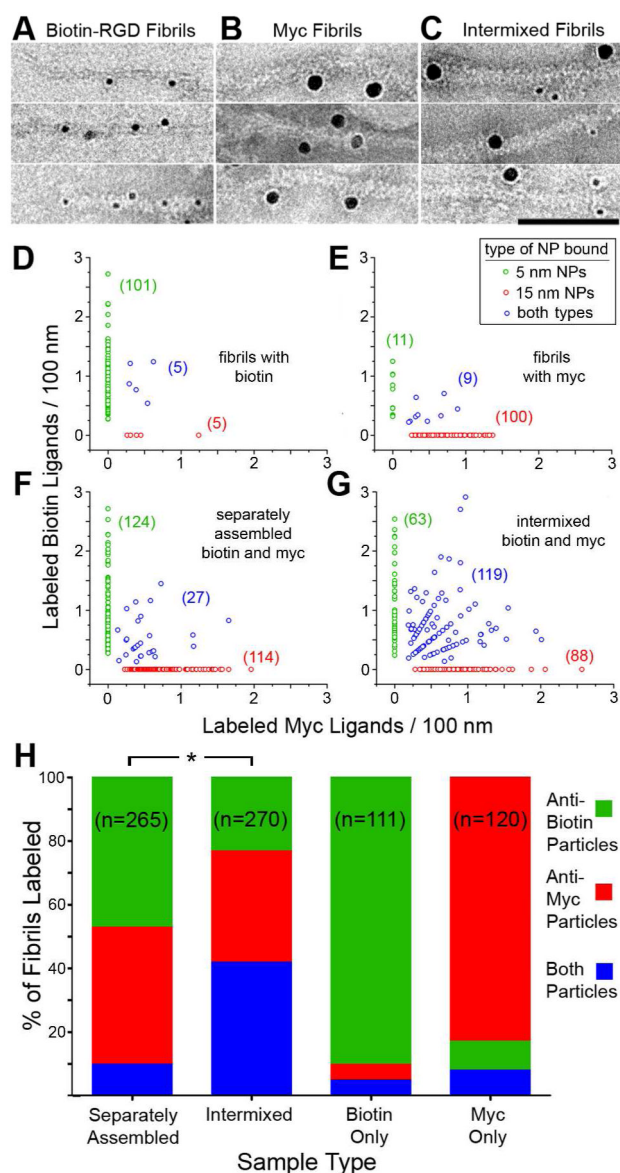
**Figure 1.**

Schematic for controlling intermixing within multi-peptide co-assemblies. (A) Table of all of peptides used (functional domain in red, fibrillizing domain in blue). In the intermixed case (B), peptides were combined in the dry state and assembled into protofibrils in water, pH 2.8. Gels were then produced by overlaying these intermixed solutions with PBS. In the separately assembled case (C), different peptides were directed to form protofibrils in water, in separate containers. These protofibrils were then mixed together and overlaid with PBS to form gels composed of distinct, unmixed fibril populations.



**Figure 2.**

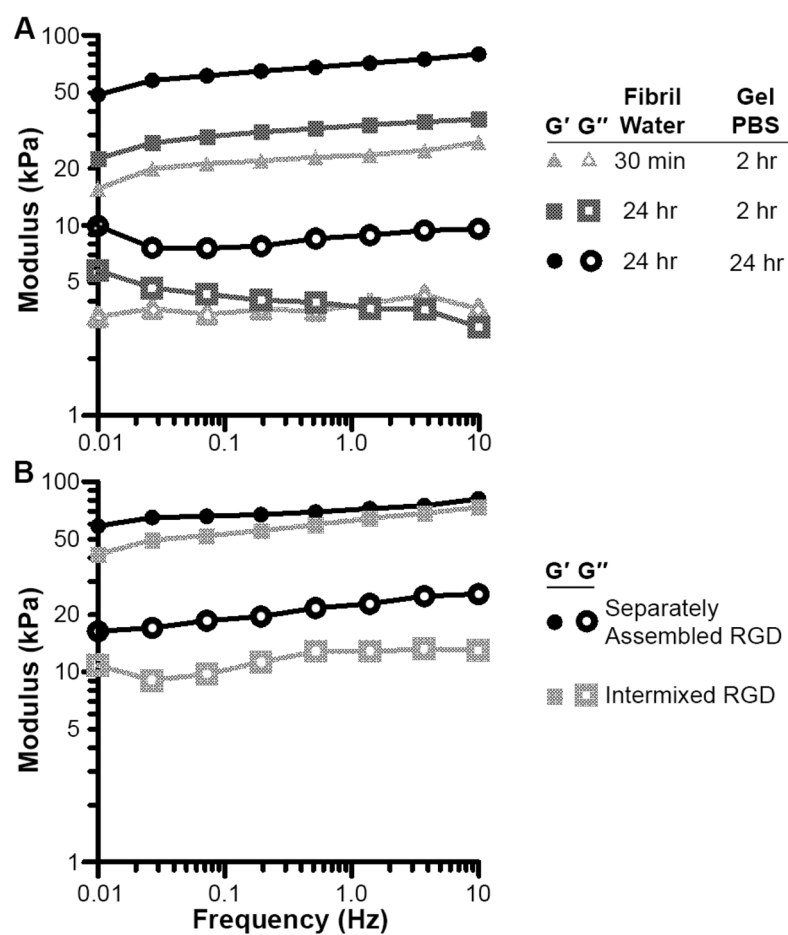
Peptides formed protofibrils in water, pH 2.8 (A, C) and mature fibrils in PBS (B). Peptide solutions were prepared in water (27 mM Q11/3 mM total ligand-bearing peptides), then diluted to 0.25 mM in either water (A) or PBS (B) and spotted onto TEM grids. Fibrils appeared wider and stained more darkly with uranyl acetate when formed in PBS (B). (C) Oscillating rheometry at 0.2% strain indicated that the storage and loss moduli of solutions of fibrils (27 mM Q11/3 mM ligand-bearing peptides as indicated) were significantly diminished compared to fully gelled Q11 peptides, which exhibit storage moduli in the range of 10–30 kPa.<sup>47</sup> ( $G'$  solid symbols,  $G''$  open symbols). Circular dichroism with the same formulations of separately assembled and intermixed peptides in water revealed beta-sheet signatures (D).



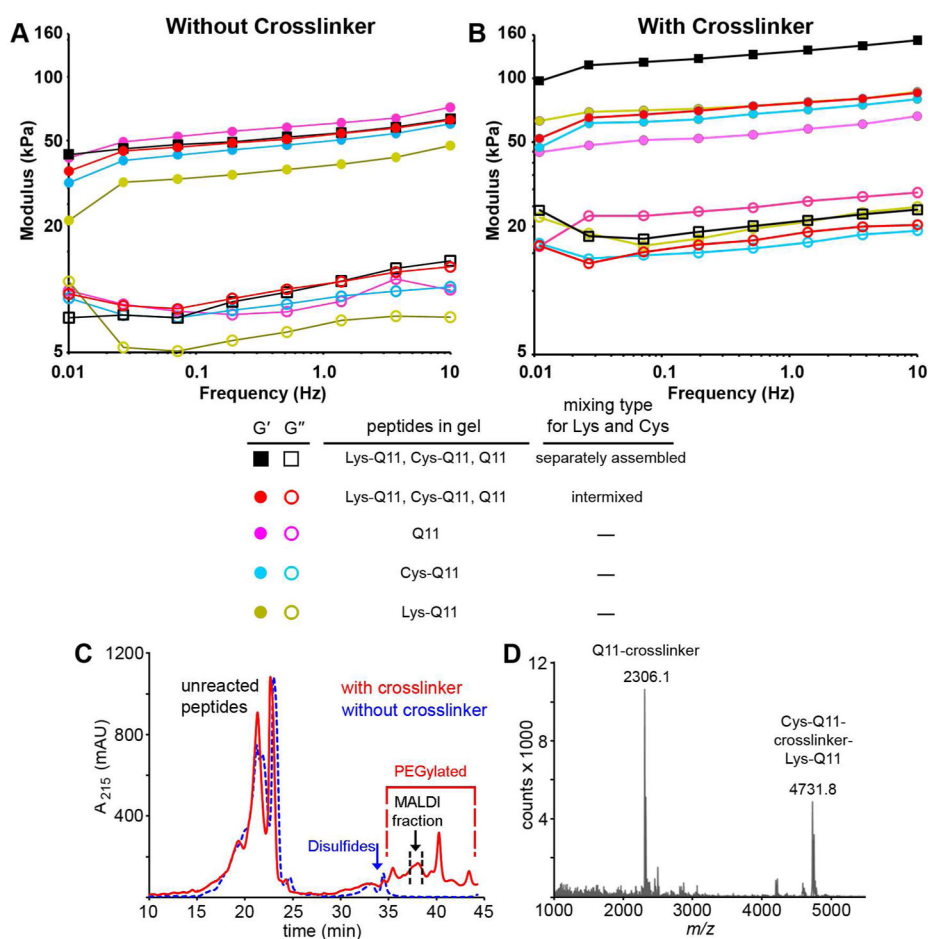
**Figure 3.** Quantification of peptide intermixing using immunoelectron microscopy. Q11 was co-assembled with biotin-RGD-Q11 (A, D), myc-Q11 (B, E), or both biotin-RGD-Q11 and myc-Q11 (C, F, G), using either intermixing or separately assembling protocols. All samples were exposed to both 5 nm gold particles specific for the biotin tags and 15 nm gold particles specific for the myc tags. Bar = 100 nm (A–C). In D–G, each data point represents a single fibril, plotted on coordinates that illustrate the number of each particle type bound per 100 nm of fibril length. Fibrils binding only biotin-specific NPs are green, fibrils binding only myc-specific NPs are red, and fibrils binding both are blue. Fibrils containing only biotin-RGD-Q11 bound predominantly biotin-specific NPs (A, D), with the opposite being true for fibrils containing only myc-Q11 (B, E). In single-label controls, the non-cognate particles bound with a background level of 9–17% (percentages shown in H, right 2 columns). Separately assembled fibrils were evenly divided into two populations binding only one of each particle type, with a similar background level (F, H, left column), whereas



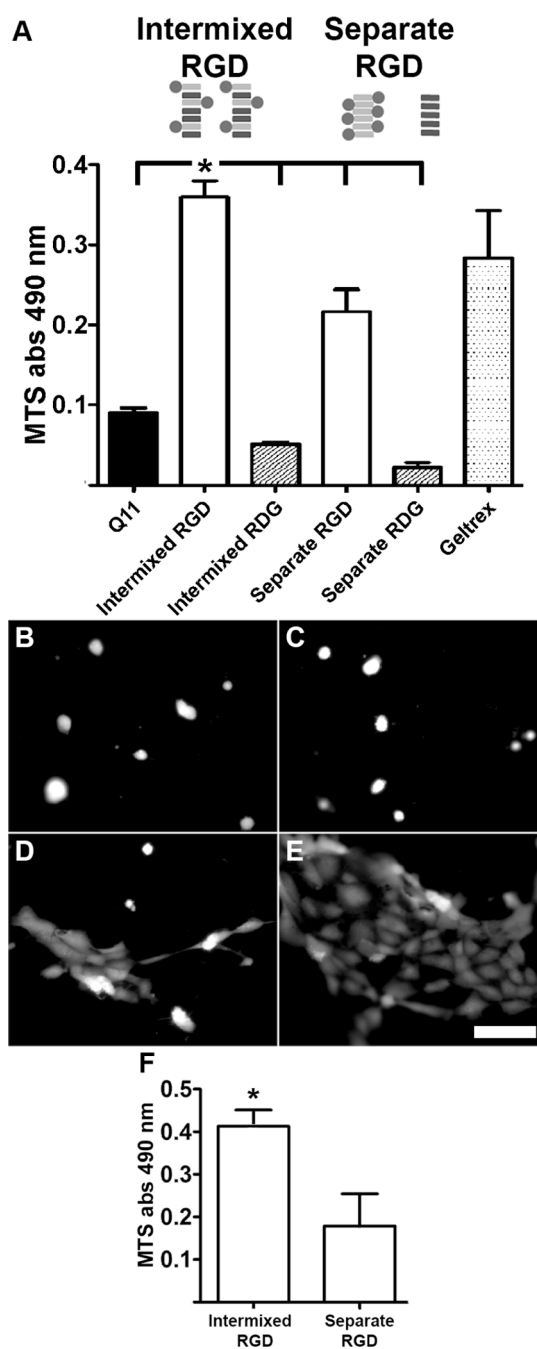
intermixed fibrils predominantly stained bound both particle types (C, G, H, left center column). \*Fisher's exact test,  $p= 2.8 \times 10^{-19}$ .



**Figure 4.** Gel viscoelasticity was dependent on the time periods allowed for protofibrillization in water and gelation in PBS (A). The degree of intermixing did not significantly influence gel storage moduli for the formulations used within cell culture experiments (B, 27 mM Q11/3 mM RGD-Q11).

**Figure 5.**

Directed intermixing can be used to control the stiffening of hydrogel assemblies. Storage and loss moduli shown for gels prior to the addition of cross-linker (A) and after (B); legend is below the data. Uncross-linked hydrogels containing separately assembled or intermixed Lys-Q11 and Cys-Q11 peptides exhibited storage moduli similar to gels made exclusively of Q11 (A). Upon application of SM(PEG)<sub>12</sub>, hydrogels containing both separately assembled Lys-Q11 and Cys-Q11 peptides stiffened to a much greater degree than all other hydrogels (B, black squares). All gels were composed of 30 mM total peptide including either 1.5 mM Cys-Q11, 1.5 mM Lys-Q11, or both. HPLC (C) and MALDI mass spectrometry (D) were used to separate PEGylated species and identify the appropriate cross-links between Cys-Q11 and Lys-Q11, respectively.

**Figure 6.**

Cell growth was significantly influenced by the intermixing of RGD ligands (27mM Q11/3mM RGD-Q11 gels, A–F). HUVEC growth (A) measured at 3 days by MTS ( $p < 0.01$ ,  $n = 3$ ). Calcein-AM stained HUVECs at day 3 on gels of Q11 (B), intermixed RGD fibrils (C), separately assembled RGD-Q11/Q11 (D), and intermixed RGD-Q11/Q11 (E). Growth of NIH 3T3 fibroblasts encapsulated within gels ( $p < 0.05$ ,  $n = 3$ ).